The effects on biomechanics of walking and balance recovery in a novel pelvis exoskeleton during zero-torque control

Dario Martelli†, Federica Vannetti‡, Mario Cortese†, Peppino Tropea†, Francesco Giovacchini†, Silvestro Micera†§, Vito Monaco†[1] and Nicola Vitiello†‡*[1]

†*The BioRobotics Institute, Scuola Superiore Sant'Anna, Pontedera, Italy*
‡*Don Carlo Gnocchi Foundation, Florence, Italy*
§*Translational Neural Engineering Lab, Center for Neuroprosthetics and Institute of Bioengineering, School of Engineering, Ecole Polytechnique Federale de Lausanne (EPFL), Lausanne, Switzerland*

SUMMARY
Fall-related accidents are among the most serious concerns in elderly people, amputees and subjects with neurological disorders. The aim of this paper was to investigate the behaviour of healthy subjects wearing a novel light-weight pelvis exoskeleton controlled in zero-torque mode while carrying out unperturbed locomotion and managing unexpected perturbations. Results showed that the proposed exoskeleton was unobtrusive and had a minimum loading effect on the human biomechanics during unperturbed locomotion. Conversely, it affected the movement of the trailing leg while subjects managed unexpected slipping-like perturbations. These findings support further investigations on the potential use of powered exoskeletons to assist locomotion and, possibly prevent incipient falls.

KEYWORDS: Rehabilitation; Exoskeletons; Man-machine systems; Perturbation; Walking.

1. Introduction
Fall-related accidents are among the most serious concerns in elderly people,[1,2] amputees[3] and subjects with neurological disorders,[4] and lead to traumatic as well as severe psychological consequences.[1] Fall-prevention programmes are hence becoming a key issue to health-care national systems, not only to reduce costs, but also to benefit society as a whole.

Many authors have provided theoretical and experimental descriptions of the biomechanics of an incipient fall revealing the high coordination patterns of upper and lower limbs while reactively managing stepping,[5,6] slipping[7−10] or tripping.[11,12] Accordingly, several interventions to reduce the risk of falls[13,14] or to mitigate the consequences of impact with the ground[15,16] have been designed and tested. Despite this, these interventions have not been as effective as desired[17] due to the intrinsic complexity of fall biomechanics, which depends on both the perturbation itself (e.g., type, direction, intensity) and on the cognitive and physical status of the persons experiencing it.

In recent years, wearable robotic orthoses, also called 'exoskeletons,' have been introduced in the field of rehabilitation robotics in order to train and/or to assist people affected by gait disorders.[18−21] These platforms, either treadmill-based or portable devices, acting on single or multiple human articulations, can actually reinforce hip, knee and/or ankle joints, assist foot placement, or entirely replace lower-limb functionalities. However, we envision that powered exoskeletons can be potentially adopted to assist locomotion and prevent falling. Indeed, exoskeletons are intrinsically provided with

* Corresponding author: E-mail: n.vitiello@sssup.it
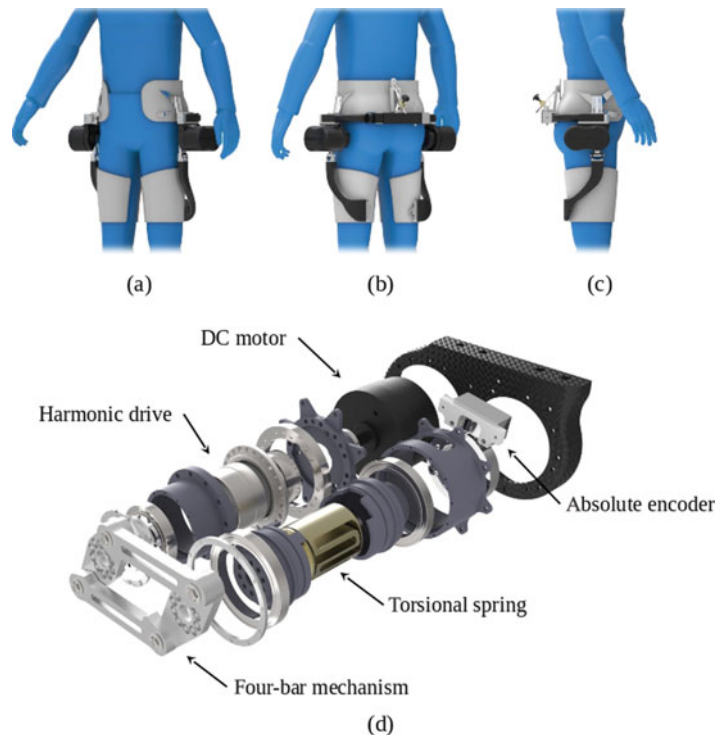[1] Equal contributors.

Fig. 1. (Colour online) CAD model of the light-weight exoskeleton: (a) front-side view; (b) back-side view; (c) lateral view; (d) actuation system.

multiple sensor platforms and actuators which could be arranged to detect incipient falls, assist unperturbed locomotion and, if necessary, supply appropriate forces (or torques) to the persons falling to help them recover their balance.

To the best of our knowledge, this hypothesis has never been systematically investigated before and there are no studies or methodologies available in literature which evaluate the interaction between users and their assistive exoskeletons following an unexpected perturbation.

The purpose of this pilot study was to analyse the biomechanics of a group of healthy subjects wearing a novel light-weight hip exoskeleton working in transparent mode (i.e., zero-torque mode) while undergoing unperturbed locomotion and managing unexpected slipping-like perturbations. Specifically, we designed this study to test the following hypotheses: (i) the biomechanics of the unperturbed locomotion of a person wearing a novel lightweight exoskeleton is not significantly modified by the robot; (ii) human–machine interaction during successful corrective reactions by healthy subjects managing unexpected slipping-like postural transitions does not significantly alter their natural motor schemes.

2. Materials and Methods

2.1. Light-weight pelvis exoskeleton
The exoskeleton used in this experiment is an active orthosis that can provide torque to the user's flexion-extension hip joint. The main features of the device, earlier presented in a conference paper,[22] are briefly recapped here for the sake of clarity. The exoskeleton (Fig. 1) is made of a carbon-fibre frame that anchors (stabilises) the entire structure over the user's body trunk through a couple of orthotic shells and carries two actuation units (one for each side). The position of the actuation units can be adjusted in order to align them with the hip flexion-extension human axes by means of two lockable sliders. Two carbon-fibre linkages are coupled to the actuation axes, which are moulded with a shape that sweeps from the lateral to the back side of the thigh: the function of each linkage is to transmit mechanical power from the motor to the respective thigh, with which it is interfaced through a custom orthotic shell. Thigh links are also endowed with a passive rotational degree of freedom (DoF) for abduction-adduction. The joint is completely passive and is not loaded by the weight of

the actuation unit, since it is placed distally with respect to the flexion-extension joint. Although the abduction-adduction axis is not aligned with the anatomical axis, it still provides comfortable interaction. The entire system has a total weight of 4.2 kg (this figure excludes the control unit which is remotely located in this prototype). This weight allowed us to consider the system light-weight, since it is known from literature that a 6-kg extra load does not affect human energy expenditure during a ground-level walking task.[23,24]

The actuation units consist of two Series Elastic Actuators (SEA)[25] whose design is centred on a custom torsional spring.[26,27] SEAs have been successfully applied in the field of wearable powered robots mainly to enhance system safety and reduce the inherent output impedance of powered joints.[19,28–30] In this case, the actuation is not rigid and allows relatively low joint impedance across the entire frequency spectrum. Furthermore, variations in the output impedance can still be achieved by means of closed-loop interaction control strategies.[25]

Each actuation unit (Fig. 1d) is configured around two parallel axes. One axis is provided with a DC motor equipped with an incremental encoder (512 counts per turn) and coupled with a Harmonic Drive (80:1 reduction ratio). The other axis (which is the actual hip joint axis) is equipped with a torsional spring in series with a 32-bit absolute encoder, which actually measures the hip joint angle. Transmission between the two parallel axes is obtained by means of a four-bar mechanism.

The control system runs on a real-time controller, a cRIO 9082 (National Instruments, Austin, Texas, US), endowed with a 1.33-GHz dual-core processor running a NI real-time operating system and a Field Programmable Gate Array (FPGA) processor Spartan-6 LX150. Motor velocity is controlled by means of a commercial servo (Maxon EPOS2 70/10). On top of the velocity control, a closed-loop 2-pole-2-zero control is used to control the joint torque. Joint torque is estimated by measuring the deformation of the torsional spring by means of the two encoders. In this regard, since the encoders have a resolution of 7.67×10^{-5} rad and the spring stiffness is 98.75 N m/rad, the resolution with which the torque is measured is in the order of 7.5×10^{-3} N m. The deformation-to-torque characteristic curve was experimentally evaluated in a previous study:[26] torque and deformation were interpolated through a linear function ($R^2 = 0.99$, RMSE $= 0.01$ N m). As a consequence, the maximum error in the estimate of torque is 0.01 N m, and actually depends on the reliability of the deformation-to-torque numerical model.

The experiments were carried out using a zero-torque control mode, i.e., with the controlled device as transparent as possible. Previous experiments aimed at assessing the performance of torque control showed that—when a healthy subject displaced the exoskeleton joint over a frequency range of 0.3–1.5 Hz—the parasitic stiffness ranged from 1 to 10 N m rad^{-1}. Furthermore, experiments with a subject walking with the exoskeleton on the treadmill showed that the passive DoFs allow comfortable interaction: the parasitic interaction torque at a cadence of about 0.7 cycle/s was indeed in the range of ± 1 N m.[22]

2.2. Participants, experimental set-up and protocol

The experimental sessions were carried out at 'Fondazione Don Carlo Gnocchi' Hospital in Florence (Italy) and involved eight young adults. Subjects were asked to perform unperturbed walking tests and to manage unexpected slipping-like perturbations: five of them (one male and four females, 37.4 ± 8.8 years old, 67.4 ± 8.2 kg, 1.70 ± 0.04 m, right dominance of the lower limb), representing the Experimental Group (EG), carried out the sessions while wearing the exoskeleton; the remaining three (one male and two females, 31.3 ± 5.1 years old, 63.0 ± 4.2 kg, 1.68 ± 0.08 m, right dominance of the lower limb), representing the Control Group (CG), carried out the sessions without wearing the exoskeleton.

All subjects were asked to walk on SENLY, a custom-made platform designed to deliver slipping-like perturbations to the subjects while walking.[31] Briefly, the device consists of two parallel and adjacent treadmills, wrapped around two platforms provided with force cells. Each treadmill can be independently moved both longitudinally and transversally to impose perturbations to the gait cycle with several combinations of kinematic parameters (i.e., maximum velocity, acceleration, rise time, hold time and fall time).

Participants had no prior experience with both the SENLY platform and the exoskeleton. The only exclusion criterion was related to subject size, due to the limited range of regulations of the orthosis prototype (i.e., pelvis width: 350–440 mm; distance between the hip joint axis and backside support: 120–175 mm).
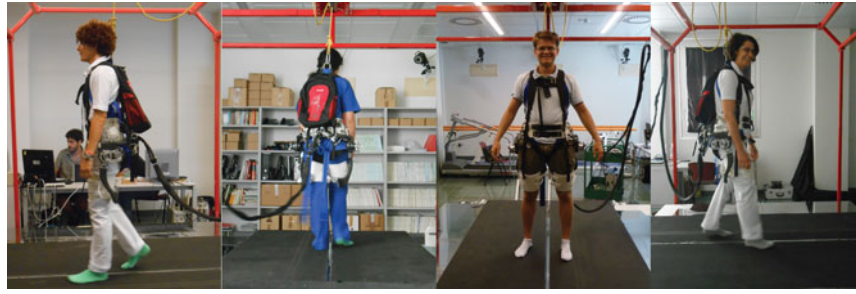
Fig. 2. (Colour online) Subjects wearing the mock-up of the pelvis exoskeleton and performing the experimental session on the SENLY platform.

Body weight, height and total leg length were recorded for each subject and dominance was determined by observing the leg he/she preferred to use while kicking a ball. Participants wore a safety harness subsequently attached to an overhead track in order to avoid impact with the ground in case of a fall (Fig. 2).

The protocol used in these experimental sessions accounted for 10 perturbations, which were provided once for each subject while walking at constant speed, and started when the left or the right heel strike was detected by SENLY. The perturbations were delivered along the anteroposterior direction with a forward movement of the treadmill on the right (i.e., North Right—NR) or the left foot (i.e., North Left—NL) at five different degrees of intensity (i.e., P1, P2, P3, P4, P5). Figure 3 shows the data of a representative slipping-like perturbation.

Five further trials, in which no perturbation was supplied, were also included in the experimental protocol. In order to obtain unbiased results:

1. participants did not know whether they would have been perturbed or not;
2. perturbations were supplied in random order;
3. data recorded during unperturbed trials were not adopted for data analysis.

As previously carried out,[10] the baseline walking speed (v) for each subject was chosen in accordance with the principle of dynamic similarity described by the Froude number (F_r), by means of the following equation:

$$v = \sqrt{F_r \cdot g \cdot L},$$

where g is the gravitational acceleration (i.e., $9.81 \mathrm{m/s^2}$) and L is the leg length from the prominence of the greater trochanter external surface to the lateral malleolus. In our case $F_r = 0.05$ was chosen to ensure safe experimental conditions.

The F_r number was also used as a metric to normalise the intensities of the perturbations for each subject (i.e., P1, P2, P3, P4, P5). In particular, five different values for the belt's maximum speed during the perturbation were defined according to a F_r ranging from 0.15 to 0.35 with a step of 0.05. All perturbations imposed a trapezoidal speed profile to a belt whose rise, hold and fall times were all set at 0.3 s. Each recording session started 1 min before delivering the perturbation while the subject was walking steadily, and ended after the subject recovered balance.

2.3. Data analysis

The EG and CG bilateral hip joint angular excursions were recorded using the exoskeleton 32-bit absolute encoders (sample rate of 1000 Hz) and a six-camera-based Vicon 512 Motion Analysis System (Davis protocol for lower limbs;[32] sample rate of 100 Hz), respectively. This choice was restricted because the exoskeleton does not allow the suitable positioning of markers on the pelvis anatomical landmarks. We hence assumed that locomotion was mainly achieved by the movements of limb segments in the plane of progression. To test the acceptability of this approximation, we compared the Range of Motion (RoM) at the hips between the two groups during unperturbed walking. Since the RoM did not significantly differ between EG and CG (see Result section, Table II), the Root Mean Square of the Difference (RMSD) of the hip joint angular excursions between
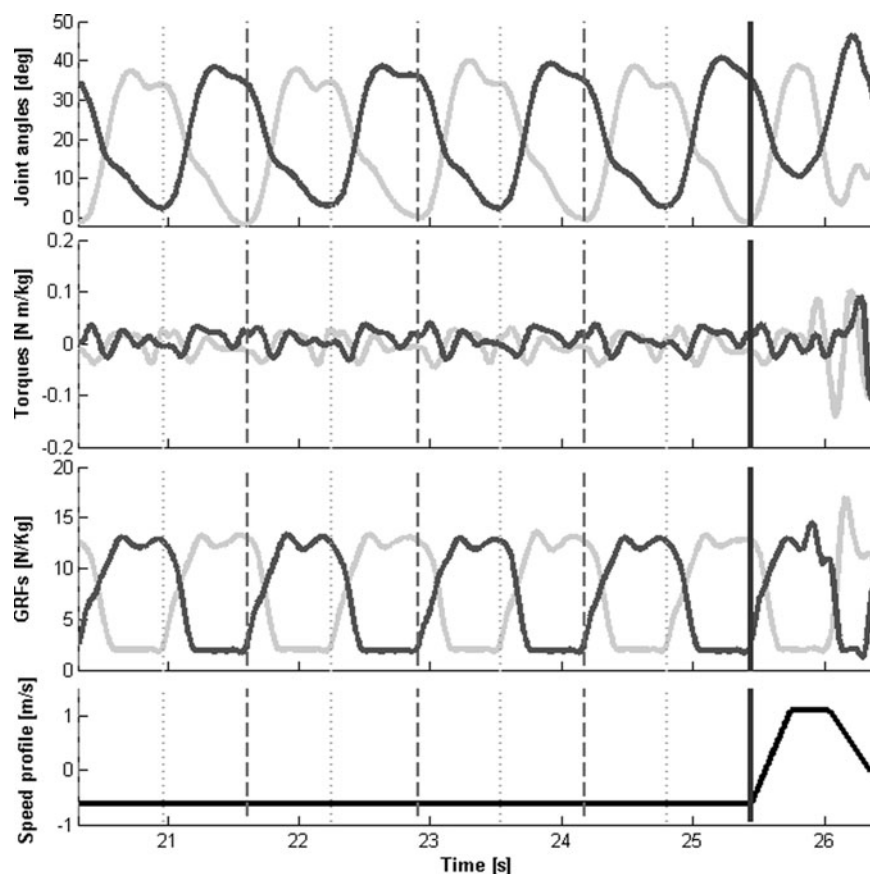
Fig. 3. A representative example of dataset recorded during a single experimental trial. From top to bottom, the subplots show the angular excursion at hip joint, the parasitic torque, the ground reaction force related to both limbs (i.e., dark and light grey curves respectively represent data obtained for the leading and the trailing leg), and the speed profile of the belt related to the perturbed side. Data refer to subject number 5 for the P1-NR perturbation. Dashed and dotted vertical lines respectively represent heel strikes of the perturbed and the unperturbed leg. The solid vertical line represents the onset of the perturbation.

the two groups related to unperturbed walking was assumed as the systematic error (i.e., accuracy) between the two measurement systems.

The bilateral hip parasitic torques delivered by the torsional spring of the series-elastic actuators of the exoskeleton were measured for the EG. In both groups, bilateral vertical ground reaction forces were measured by SENLY at a sampling rate of 1000 Hz. All systems were synchronised by means of a logic pulse generated by SENLY while delivering the perturbation.

For each subject and each trial, data were subdivided into two subsets: data recorded before and after the onset of the perturbation. The former referred to the last five ipsilateral unperturbed strides, in which each cycle started with the heel strike of the leg being perturbed. These data were divided into strides, individually time-interpolated over 101 points, and averaged in order to have a representative gait cycle. In this case, only data related to the ipsilateral leg (with respect to the side of the perturbation) were analysed. The latter referred to the compensatory step, in which each cycle started simultaneously with the onset of the perturbation (i.e., the heel strike of the leading/perturbed leg) and finished with the heel strike of the trailing/unperturbed leg. Data related to the compensatory step were also time-interpolated over 101 points. In this case, both data related to the leading and trailing leg were analysed.

In order to verify the effect of the exoskeleton on human kinematics, hip joint angular excursions related to the EG and the CG were compared by using three metrics: the RoM, the RMSD and the Pearson correlation coefficient (ρ).

In both motor tasks, the exoskeleton was considered transparent if the RoM was not significantly different between EG and CG and the ρ was higher than 0.90. During perturbations, the exoskeleton

Table I. Subjects' anthropometric measures and walking speed.

Group	Subject	Weight [kg]	Height [m]	Leg length [m]	Age [years]	Speed [m/s]	Gender	Dominance
EG	1	58	1.7	0.84	47	0.64	F	Right
	2	75	1.75	0.81	29	0.63	M	Right
	3	72	1.72	0.79	47	0.62	F	Right
	4	59	1.67	0.81	32	0.63	F	Right
	5	73	1.65	0.8	32	0.63	F	Right
	Mean	67.4	1.70	0.81	37.4	0.63		
	S.D.	8.2	0.04	0.02	8.9	0.01		
CG	6	64	1.7	0.86	37	0.65	F	Right
	7	67	1.75	0.85	30	0.65	M	Right
	8	58	1.6	0.8	27	0.63	F	Right
	Mean	63	1.68	0.84	31.3	0.64		
	S.D.	4.6	0.08	0.03	5.1	0.01		

was considered transparent also if the duration of the compensatory step was not significantly different between EG and CG and the RMSD was not significantly different from that measured during unperturbed locomotion (i.e., accuracy). The Kolmogorov–Smirnov test with Lilliefors correction was performed to check the normality assumption of the data. After that, the *F*-test of equality of variances was performed to check the homoscedasticity of the accounted levels. Then, for each perturbation, unpaired *t*-tests were performed to compare the RoMs and the duration of the compensatory step obtained by the EG and the CG, while one-sample *t*-tests were used to compare the RMSDs obtained during the perturbations with those measured during unperturbed locomotion.

In order to verify the effect of the perturbation on human kinetics while the subjects were wearing the exoskeleton (i.e., the EG), the pick of the hip parasitic torques felt by the leading and the trailing leg during the perturbations were compared to that obtained during unperturbed walking by means of unpaired *t*-tests. Data analysis was carried out using custom Matlab (The MathWorks, Inc., Natick, MA, USA) scripts. Significance was set at $\alpha = 0.05$.

3. Results

3.1. Hip joint angular excursion and torque during unperturbed walking

The anthropometric measures of each subject are reported in Table I.

EG and CG paces were characterised by comparable features: walking speed was 0.63 ± 0.01 m/s for the EG and 0.64 ± 0.01 m/s for the CG; the duration of the gait cycle was 1.33 ± 0.11 s for the EG and 1.38 ± 0.05 s for the CG.

Figure 4 shows the hip joint angular excursion during one gait cycle (the mean trajectory—solid line—was reported along with one standard deviation contour—shadowed) while subjects were (light grey curve) and were not (dark grey curve) wearing the exoskeleton.

From a qualitative viewpoint, these kinematic patterns were very similar between the groups, even though the hip excursions related to the EG were characterised by a slight shift towards positive values. More in detail, analysis of the angular excursions revealed that the shape of the hip joint angular excursion was very similar between the two experimental conditions (ρ was on average 0.97 ± 0.02) and the RoM did not significantly ($p > 0.05$) differ between EG and CG (Table II). Accordingly, the exoskeleton could be considered transparent under the considered assumption and the systematic error between the two measurement systems was 6.0 deg (see RMSD in Table II).

The torque measured by the exoskeleton on average ranged between –0.03 and 0.03 N m/kg (Fig. 4). It assumed lower values (on average, within ±0.01 N m/kg) during most of the stance phase and increased when the hip started to flex (about 50% of the gait cycle).

Table II. Range of Motion (RoM), Root Mean Square of the Difference (RMSD), and Pearson correlation coefficient (ρ) of the hip joint angular excursion during the gait cycle while subjects were (Experimental Group—EG) and were not (Control Group—CG) wearing the exoskeleton. When the *p*-value is statistically significant ($p < 0.05$), it is highlighted in bold.

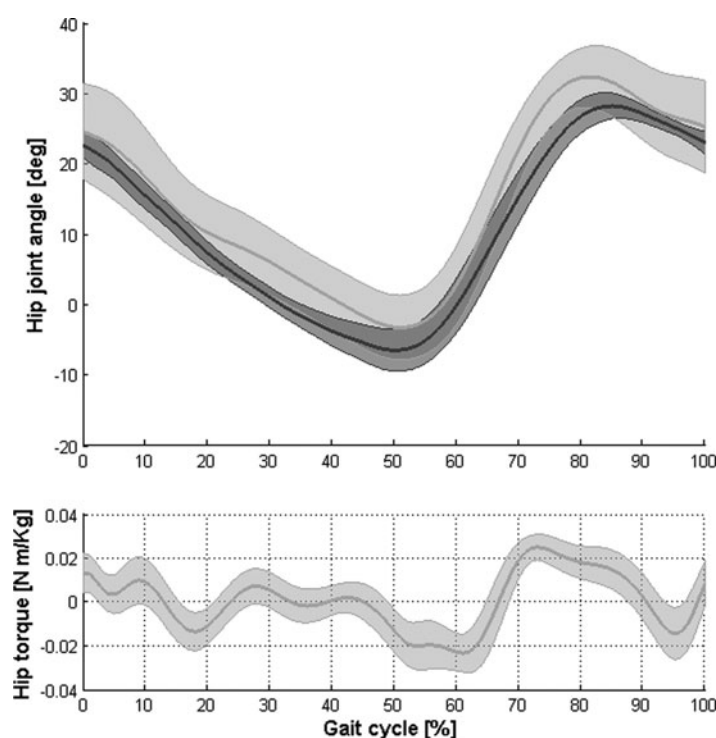| | | RoM [deg] | | |
| | | Groups | | |
ρ	RMSD [deg]	EG	CG	p-value
0.97 ± 0.02	6.0 ± 3.1	36.0 ± 2.1	34.9 ± 2.8	0.61

Fig. 4. Mean and one standard deviation (error band) of hip joint angular excursion (top) and the parasitic torque (bottom) during the gait cycle while subjects were (Experimental Group—EG—light grey curves) and were not (Control Group—CG—dark grey curves) wearing the exoskeleton. Mean values refer to the average of the last five ipsilateral unperturbed strides for all the subjects.

3.2. Hip joint angular excursion and torque during the perturbation

All participants were able to manage the unexpected perturbations and recover their balance without falling. Homologous data related to left and right perturbations (i.e., NR and NL) were pooled for each degree of intensity because no significant effect of the side (i.e., right and left feet) was ever observed.

Figure 5 shows the duration of the compensatory cycle while subjects were (light grey bars) and were not (dark grey bars) wearing the exoskeleton, for all the intensities of perturbation.

Results showed that the duration of the compensatory cycle was comparable ($p > 0.05$ for all the perturbations) between the EG (on average 0.48 ± 0.1 s) and the CG (on average 0.41 ± 0.08 s).

Figure 6 shows hip joint angular excursion related to the leading (left side) and the trailing (right side) limbs during the compensatory step while subjects were (light grey curves) and were not (dark grey curves) wearing the exoskeleton. To make reading easier, only data related to the lowest and the highest intensities of perturbation (i.e., P1 and P5) were reported.
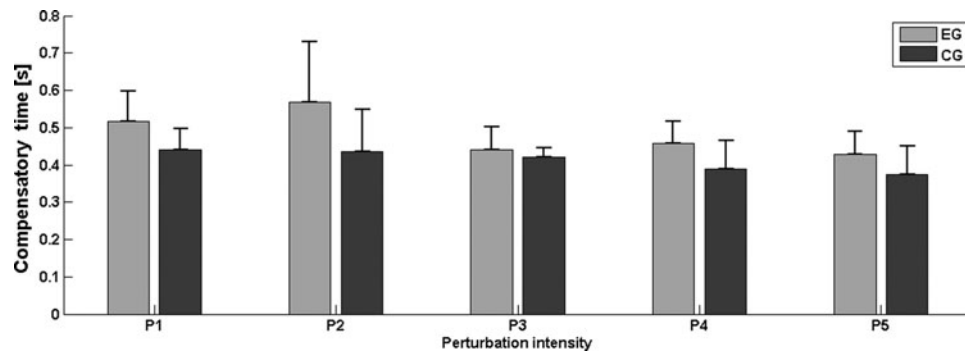
Fig. 5. Mean and one standard deviation (error band) of the duration of the compensatory cycle while subjects were (Experimental Group—EG—light grey bars) and were not (Control Group—CG—dark grey bars) wearing the exoskeleton, for all the perturbations (P1, P2, P3, P4 and P5). The compensatory cycle was defined as the time that lasted from the onset of the perturbation (i.e., the heel strike of the perturbed/leading leg) and the heel strike of the unperturbed/trailing leg.
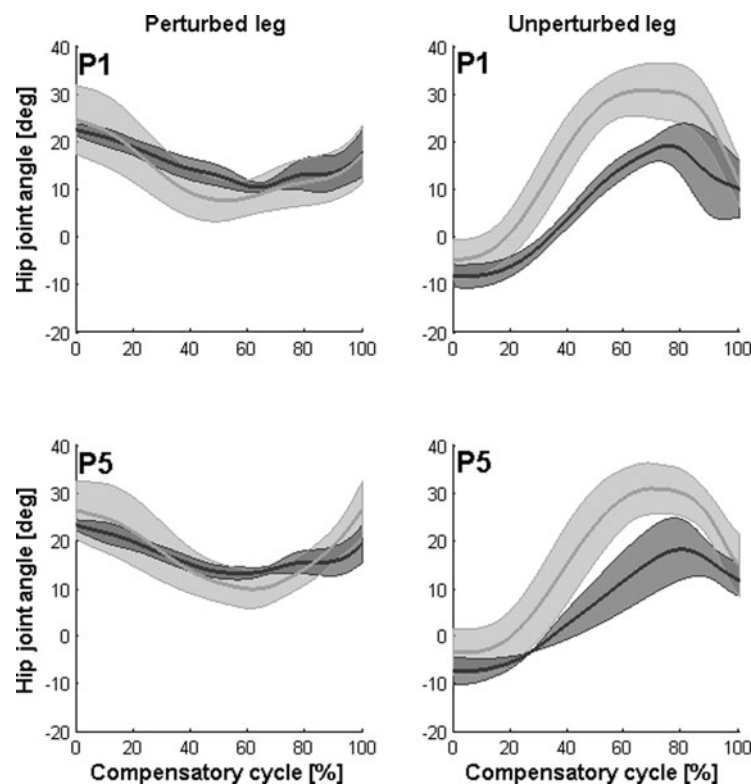

Fig. 6. Mean and one standard deviation (error band) of hip joint angular excursion during the compensatory cycle of the perturbed/leading (on the left) and the unperturbed/trailing (on the right) leg while subjects were (Experimental Group—EG—light grey curves) and were not (Control Group—CG—dark grey curves) wearing the exoskeleton. To make reading easier, only data related to the lowest and the highest intensities of perturbations (i.e., P1 and P5) were reported. The compensatory cycle was defined as the time that lasted from the onset of the perturbation (i.e., the heel strike of the leading leg) and the heel strike of the trailing leg.

Results revealed that after the onset of the perturbation, the hip extension of the leading leg was stopped due to the forward movement of the belt while the trailing limb was rapidly flexed to achieve the compensatory step (Figs. 4 and 6).

Table III reports the ρ and the RMSD obtained during all the perturbations (i.e., P1–P5) for both the trailing and leading leg. Noticeably, the EG and CG hip kinematics related to both limbs were quite similar in terms of shape for all the perturbations (ρ ranges between 0.71 and 0.94). The RMSDs

Table III. Root Mean Square of the Difference (RMSD) and Pearson correlation coefficient (ρ) of the hip joint angular excursion during the compensatory cycle while subjects were (Experimental Group—EG) and were not (Control Group—CG) wearing the exoskeleton. When the *p*-value is statistically significant ($p < 0.05$), it is highlighted in bold.

Leg	Intensity	ρ	RMSD [deg]	*p*-value
Perturbed	P1	0.86 ± 0.17	5.8 ± 2.4	0.82
	P2	0.71 ± 0.50	6.9 ± 3.6	0.5
	P3	0.89 ± 0.09	5.2 ± 2.0	0.36
	P4	0.93 ± 0.05	5.4 ± 2.8	0.62
	P5	0.89 ± 0.05	5.2 ± 3.1	0.53
	Mean	0.86 ± 0.24	5.7 ± 2.7	
Unperturbed	P1	0.92 ± 0.07	12.4 ± 3.3	**<0.05**
	P2	0.86 ± 0.16	13.6 ± 3.6	**<0.05**
	P3	0.90 ± 0.06	11.8 ± 4.1	**<0.05**
	P4	0.94 ± 0.04	11.4 ± 2.9	**<0.05**
	P5	0.93 ± 0.05	12.3 ± 3.7	**<0.05**
	Mean	0.91 ± 0.09	12.3 ± 3.4	

Table IV. Range of Motion (RoM) of the hip joint angular excursion during the compensatory cycle while subjects were (Experimental Group—EG) and were not (Control Group—CG) wearing the exoskeleton. When the *p*-value is statistically significant ($p < 0.05$), it is highlighted in bold.

		RoM [deg]		
		Groups		
Leg	Intensity	EG	CG	*p*-value
Perturbed	P1	18.4 ± 4.5	12.6 ± 1.0	0.06
	P2	18.7 ± 5.9	15.5 ± 6.4	0.4
	P3	16.0 ± 3.9	12.6 ± 0.8	0.19
	P4	17.5 ± 3.9	11.6 ± 1.3	**<0.05**
	P5	18.6 ± 5.5	10.6 ± 2.0	**<0.05**
	Mean	17.8 ± 4.6	12.6 ± 3.4	
Unperturbed	P1	37.4 ± 5.0	28.6 ± 0.8	**<0.05**
	P2	39.5 ± 8.7	30.8 ± 4.6	0.1
	P3	35.4 ± 3.3	29.2 ± 7.2	0.08
	P4	37.1 ± 4.8	26.4 ± 3.1	**<0.05**
	P5	35.1 ± 1.8	27.3 ± 8.9	**<0.05**
	Mean	36.9 ± 5.2	28.5 ± 5.0	

related to the perturbed leg were always comparable with the measure accuracy ($p > 0.05$). By contrast the RMSDs related to the trailing leg were always greater than the measure accuracy ($p > 0.05$).

The RoMs obtained during all the perturbations (i.e., P1–P5) for both legs (i.e., trailing and leading) and groups (i.e., EG and CG) were reported in Table IV. Results revealed that for both legs and almost all intensities of perturbations, the RoMs in the EG were significantly ($p < 0.05$) greater than in the CG. According to these results, hip kinematics seems to be quite affected by the presence of the exoskeleton during the recovery phase, above all for the trailing leg.

Figure 7 shows the parasitic torque measured by the exoskeleton on the leading (left side) and the trailing (right side) limbs during the compensatory step. To make reading easier, only data related to the lowest and the highest intensities of perturbation (i.e., P1 and P5) were reported.

Torques were relatively small and ranged between –0.05 and 0.02 N m/kg (Fig. 7—left side) in the perturbed leg, and between –0.1 and 0.1 N m/kg (Fig. 7—right side) in the unperturbed leg. In particular, the intrinsic mechanical impedance of the exoskeleton seems to increase consistently due to the rapid compensatory step of the unperturbed leg.
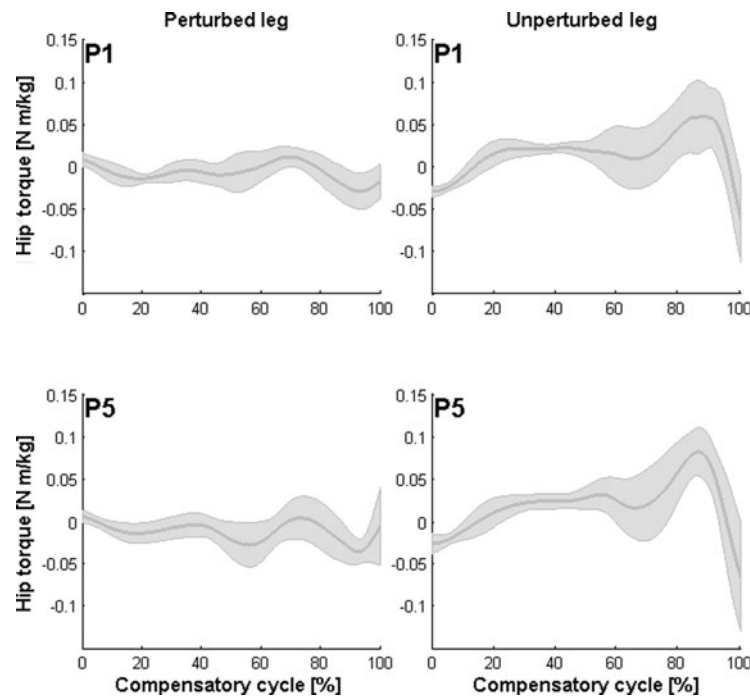
Fig. 7. Mean and one standard deviation (error band) of hip parasitic torque during the compensatory cycle of the perturbed/leading (on the left) and the unperturbed/trailing (on the right) leg while subjects (Experimental Group—EG) were wearing the exoskeleton. To make reading easier, only data related to the lowest and the highest intensities of perturbations (i.e., P1 and P5) were reported. The compensatory cycle was defined as the time that lasted from the onset of the perturbation (i.e., the heel strike of the leading leg) and the heel strike of the trailing leg.

Figure 8 shows the peak of the parasite torque felt by the leading (on the top) and the trailing (on the bottom) legs during the compensatory cycle while subjects were wearing the exoskeleton. Results revealed that, for both legs, the peak of the parasite torque during the perturbations was almost always significantly ($p < 0.05$) greater than that measured during unperturbed walking.

4. Discussion

This pilot study aimed at investigating the behaviour of subjects wearing a novel exoskeleton controlled in zero-torque mode while carrying out unperturbed locomotion and managing unexpected slipping-like perturbations. The results of this work provide insights into the design and development of a light-weight exoskeleton which is expected to assist locomotion and effectively contribute to the recovery of balance in persons prone to falling. Indeed, this is one of the main scientific goals which are expected to be achieved within the CYBERLEGs project[2]. This project aims to develop an artificial cognitive ortho-prosthesis system[33] for the replacement of the lost limb of dysvascular transfemoral amputees and to provide assistance to the sound limb. The final prototype is expected to allow amputees to walk, climb stairs and move from sit-to-stand and stand-to-sit with limited cognitive and energetic effort. Finally, in order to encourage the amputee to rely on the prosthesis, the CYBERLEGs orthosis will also have the role of detecting incipient falls and providing the amputee legs with extra power to mitigate their risk of fall.

With reference to the investigation of strategies to address incipient fall detection and balance recovery through active exoskeletons, the main challenge is to evaluate whether the powered wearable robot can actually affect user biomechanics. The hypothesis here was that the proposed light-weight exoskeleton was unobtrusive and had a minimum loading effect on human biomechanics both during

---

[2] CYBERLEGs (namely "The CYBERnetic LowEr-Limb CoGnitive Ortho-prosthesis") is a European FP7-ICT Project; the project started on February 2012 and will last three years. More details are available at: www.cyberlegs.eu.
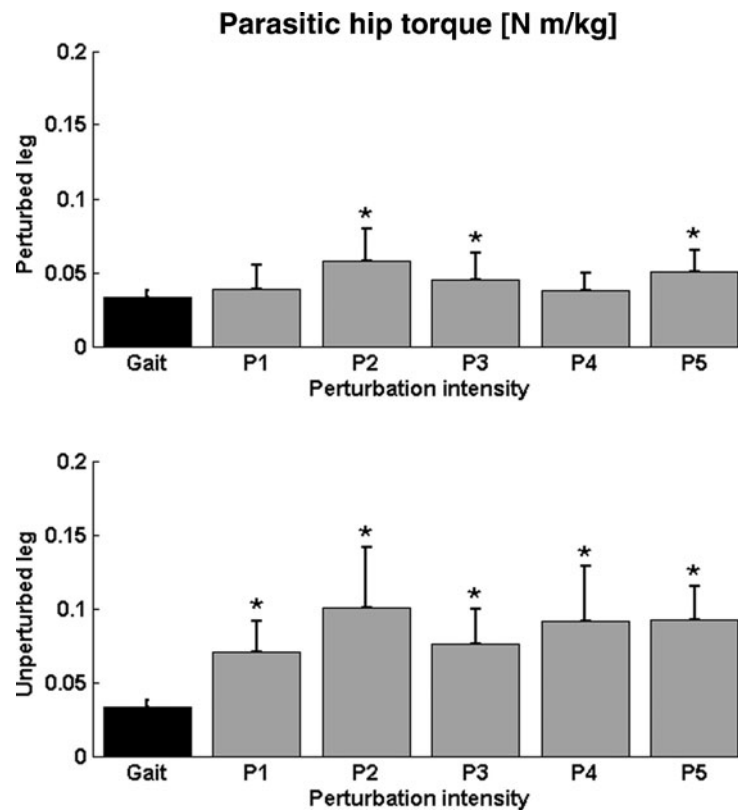
Fig. 8. Mean and one standard deviation (error bar) of the absolute value of the peak of the parasitic torque felt by the leading/perturbed (on the top) and the trailing/unperturbed (on the bottom) legs during the compensatory cycle while subjects (Experimental Group—EG) were wearing the exoskeleton. Data in black refer to the unperturbed locomotion. The label '∗' on the top of each bar indicates a significant difference ($p < 0.05$) between values measured during the unperturbed walking and those referring to the compensatory cycle.

steady-state locomotion and slipping-like perturbations. The minimum loading effect of the orthosis on human biomechanics is indeed desirable in order to ground the investigation and development of incipient-fall detection and balance recovery strategies for amputees in the light of extensive existing literature.[15,16,34] Furthermore, we know from literature that an orthosis can affect human biomechanics mostly in terms of kinematic constraints as well as of resistive torques applied on the human articulations, the latter being the result of inherent gear-head motor inertia, transmission friction and limited closed-loop control bandwidth.[18,19,33]

The results of this work—as discussed below—actually showed that the mechanics, actuation unit and control system of the proposed pelvis exoskeleton were unobtrusive and had a minimum loading effect on human biomechanics during unperturbed steady-state locomotion while seemed to affect the recovery responses elicited by subjects during unexpected slipping-like perturbations. Specifically, the workload of the trailing leg increased during the rapid achievement of the compensatory step in order to counteract the resistive, parasitic torque of the exoskeleton joints.

4.1. Human–robot interaction during unperturbed steady-state locomotion
The results reported in Fig. 4 and Table II show that during the steady-state gait the proposed light-weight orthosis did not significantly affect the human gait. All of the subjects could easily wear the exoskeleton and did not report any discomfort during the experimental tests. Hip joint kinematics was only slightly modified by the presence of the exoskeleton: the hip trajectories recorded in subjects that did not wear the exoskeleton were actually comparable to those of subjects wearing the exoskeleton. This was proved by the fact that the hip joint angular excursions were very well correlated (ρ was on average 0.97 ± 0.02) and the RoMs between the two groups were comparable ($p > 0.05$; see Table II).

The slight discrepancy observed between the two groups reflects both ergonomic-related reasons and the specific strategies taken by the subjects to react to the exoskeleton's small, still-not-null loading effect (Fig. 4). In particular, subjects seemed to slightly increase hip flexion during the swing phase in order to counteract the load induced by the exoskeleton. This strategy, therefore, might have led the subjects to increase concentric hip power during the late stance. However, it is worth noting that the loading effect of the exoskeleton on hip kinematics was actually minimal due to two features of the proposed exoskeleton. First, the inertia of the carbon-fibre linkages was very low compared to that of the human thigh. Second, the parasitic, resistive torque applied by the actuation units onto the human joint had quite low values: the peak resistive torque was about 0.02 N m/kg, i.e., 1.4 N m for a 70-kg subject, which corresponds to about 2% of the hip flexion-extension peak torque during ground-level walking at normal cadence.[35]

4.2. Human–robot interaction during slipping-like perturbations

All subjects successfully managed unexpected slipping-like postural transitions, even though results showed that the exoskeleton was slightly encumbered by the recovery responses elicited by the subjects.

The main challenge here was the risk that an excessive resistive torque—elicited by faster human movements following the slipping-like perturbation—could prevent the subject from successfully recovering balance. Indeed, with an increasing frequency content in the joint movement, the series-elastic actuator output impedance progressively increases towards its maximum value, i.e., the inherent stiffness of the series torsional spring. An increasing output impedance would be hence responsible for a higher resistive torque.

Actually, the resistive torque felt by the trailing leg was higher as a consequence of a faster swing (which is the normal strategy humans adopt to prevent from slipping), and reached a peak value on the trailing leg of about 0.1 N m/kg, i.e., 7 N m for a 70-kg subject, which corresponds to about 20% of the hip flexion-extension peak torque during ground-level walking at normal cadence[35] (Figs. 7 and 8).

Despite the higher resistive torque, the hip joint angular excursion related to the trailing leg showed that the swing phase was successfully accelerated (Fig. 6—right side) and the stable double support was achieved timely, as demonstrated by the fact that the duration of the compensatory cycle is comparable between the EG and the CG. This result demonstrated that the series-elastic actuation solution—and the related zero-torque control mode—is a suitable architecture for exoskeletons that have to both assist the human joints and possibly detect the incipient fall.

It is worth noting that the larger effort (about 20% higher peak of hip flexion-extension torque) that subjects were required to apply to counteract the resistive torque of the exoskeleton joints and timely achieve the compensatory step is not a limiting factor when using the exoskeleton to mitigate the risk of fall. Indeed, as an ultimate goal of our study, we expect the exoskeleton to detect the incipient fall online and consequently mitigate the risk of fall by providing the amputee with an assistive torque—via tracking of a torque reference different from null—which will help recover a stable support.

4.3. Limitations of this study

This study was mainly limited by two facts. First, owing to the small number of participants, the statistical findings were not strong. Second, the walking speed was, on average, 0.63 m/s which can be considered quite slow compared to the preferred walking speed of young and healthy subjects. On the one hand, the slow speed contributed to corroborating the assumption that locomotion was mainly achieved by the movements of the limb segments in the plane of progression in order to allow a straightforward comparison of the kinematics between the two measurement systems. On the other hand, it was a consequence of the safety constraints we wished to address in this preliminary study: specifically, we wished to reduce any risks of injury for the user resulting from possible failure of the prototype caused by excessive resistive torque generated by concomitant high joint velocity (as a consequence of a higher gait velocity) and joint accelerations for balance-recovery. However, this study is the first in which slipping-like perturbations were imposed while subjects donned an active orthosis powered by SEAs under zero-torque control mode. It represents a suitable model to test and validate the effectiveness of similar platforms designed to both assist locomotion and prevent falling.

5. Conclusions

Reported preliminary results confirm that, during unperturbed locomotion, the proposed light-weight exoskeleton can reasonably be considered transparent while working in zero-torque mode. Moreover, they provide normative data describing the kinematics of the compensatory step used to recover loss of balance while healthy adults wear the pelvis exoskeleton controlled in transparent mode.

Future works will mostly aim at investigating a strategy for recognising and preventing the incipient fall of the amputee, within the framework of the CYBERLEGs project. Specifically, we will aim at designing suitable strategies capable of detecting an incipient fall early enough to provide supplementary forces to regain stability and minimise the risk of impact by the subject with the ground. Dedicated experimental sessions will be carried out to achieve this final goal. On the whole, these results can be used as a basis for establishing suitable parameters to be implemented in orthosis control once the incipient falling is detected.

References

1. T. Masud and R. O. Morris, "Epidemiology of falls," *Age and Ageing* **30**(4), 3–7 (2001).
2. W. P. Berg, H. M. Alessio, E. M. Mills and C. Tong, "Circumstances and consequences of falls in independent community-dwelling older adults," *Age Ageing* **26**(4), 261–268 (1997).
3. W. C. Miller, M. Speechley and B. Deathe, "The prevalence and risk factors of falling and fear of falling among lower extremity amputees," *Arch. Phys. Med. Rehabil.* **82**(8), 1031–1037 (2001).
4. H. Stolze, S. Klebe, C. Zechlin, C. Baecker, L. Friege and G. Deuschl, "Falls in frequent neurological diseases–prevalence, risk factors and aetiology," *J. Neurol.* **251**(1), 79–84 (2004).
5. M. H. van der Linden, D. S. Marigold, F. J. Gabreels and J. Duysens, "Muscle reflexes and synergies triggered by an unexpected support surface height during walking," *J. Neurophysiol.* **97**(5), 3639–3650 (2007).
6. D. S. Marigold and A. E. Patla, "Adapting locomotion to different surface compliances: Neuromuscular responses and changes in movement dynamics," *J. Neurophysiol.* **94**(3), 1733–1750 (2005).
7. P. F. Tang, M. H. Woollacott and R. K. Chong, "Control of reactive balance adjustments in perturbed human walking: Roles of proximal and distal postural muscle activity," *Exp. Brain Res.* **119**(2), 141–152 (1998).
8. B. E. Moyer, M. S. Redfern and R. Cham, "Biomechanics of trailing leg response to slipping – Evidence of interlimb and intralimb coordination," *Gait Posture* **29**(4), 565–570 (2009).
9. D. S. Marigold, A. J. Bethune and A. E. Patla, "Role of the unperturbed limb and arms in the reactive recovery response to an unexpected slip during locomotion," *J. Neurophysiol.* **89**(4), 1727–1737 (2003).
10. D. Martelli, V. Monaco, L. Bassi Luciani and S. Micera, "Angular momentum during unexpected multidirectional perturbations delivered while walking," *IEEE Trans. Biomed. Eng.* **60**(7), 1785–1795 (2013).
11. M. Pijnappels, M. F. Bobbert and J. H. van Dieen, "Contribution of the support limb in control of angular momentum after tripping," *J. Biomech.* **37**(12), 1811–1818 (2004).
12. J. J. Eng, D. A. Winter and A. E. Patla, "Strategies for recovery from a trip in early and late swing during human walking," *Exp. Brain Res.* **102**(2), 339–349 (1994).
13. A. Mansfield, A. L. Peters, B. A. Liu and B. E. Maki, "Effect of a perturbation-based balance training program on compensatory stepping and grasping reactions in older adults: A randomized controlled trial," *Phys. Ther.* **90**(4), 476–491 (2010).
14. P. Parijat and T. E. Lockhart, "Effects of moveable platform training in preventing slip-induced falls in older adults," *Ann. Biomed. Eng.* **40**(5), 1111–1121 (2012).
15. M. N. Nyan, F. E. Tay and E. Murugasu, "A wearable system for pre-impact fall detection," *J. Biomech.* **41**(16), 3475–3481 (2008).
16. G. Wu and S. Xue, "Portable preimpact fall detector with inertial sensors," *IEEE Trans. Neural Syst. Rehabil. Eng.* **16**(2), 178–183 (2008).
17. S. M. Bruijn, O. G. Meijer, P. J. Beek and J. H. van Dieen, "Assessing the stability of human locomotion: A review of current measures," *J. R. Soc. Interface* **10**(83), 20120999 (2013).
18. J. L. Pons, "Rehabilitation exoskeletal robotics. The promise of an emerging field," *IEEE Eng. Med. Biol. Mag.* **29**(3), 57–63 (2010).
19. J. F. Veneman, R. Kruidhof, E. E. G. Hekman, R. Ekkelenkamp, E. H. F. Van Asseldonk and H. van der Kooij, "Design and evaluation of the LOPES exoskeleton robot for interactive gait rehabilitation," *IEEE Trans. Neural Syst. Rehabil. Eng.* **15**(3), 379–386 (2007).
20. A. M. Dollar and H. Herr, "Lower extremity exoskeletons and active orthoses: Challenges and state-of-the-art," *IEEE Trans. Robot.* **24**(1), 144–158 (2008).

21. R. J. Farris, H. A. Quintero and M. Goldfarb, "Performance Evaluation of a Lower Limb Exoskeleton for Stair Ascent and Descent with Paraplegia," *Proceedings of the Annual International Conference of the IEEE Engineering in Medicine and Biology Society (EMBC)*, San Diego, CA, USA (Aug. 28–Sep. 1, 2012) pp. 1908–1911.
22. F. Giovacchini, M. Fantozzi, M. Peroni, M. Moisé, M. Cempini, M. Cortese, D. Lefeber, M. C. Carrozza and N. Vitiello, "A Light-weight Exoskeleton for Hip Flexion-extension Assistance," *Proceedings of the 1st International Congress on Neurotechnology, Electronics and Informatics*, Vilamoura, Portugal (Sep. 18–20, 2013) pp. 194–198.
23. D. Abe, K. Yanagawa and S. Niihata, "Effects of load carriage, load position, and walking speed on energy cost of walking," *Appl. Ergon.* **35**(4), 329–335 (2004).
24. P. E. Martin and R. C. Nelson, "The effect of carried loads on the walking patterns of men and women," *Ergonomics* **29**(10), 1191–1202 (1986).
25. G. A. Pratt and M. M. Williamson, "Series Elastic Actuators Iros '95," *Proceedings of the IEEE/RSJ International Conference on Intelligent Robots and Systems: Human Robot Interaction and Cooperative Robots*, Pittsburgh, PA, USA (Aug. 5–9, 1995) pp. 399–406.
26. M. Cempini, F. Giovacchini, N. Vitiello, M. Cortese, M. Moise, F. Posteraro and M. C. Carrozza, "NEUROExos: A Powered Elbow Orthosis for Post-Stroke Early Neurorehabilitation," *Proceedings of the Annual International Conference of the IEEE Engineering in Medicine and Biology Society*, Osaka, Japan (Jul. 3–7, 2013) pp. 342–345.
27. F. Giovacchini, M. Cempini, N. Vitiello and M. C. Carrozza, *Molla Torsionale*, Italian Patent Application, Application number: FI2013A000156, Application date: July 1, 2013.
28. N. Vitiello, T. Lenzi, S. Roccella, S. M. M. De Rossi, E. Cattin, F. Giovacchini, F. Vecchi and M. C. Carrozza, "NEUROExos: A powered elbow exoskeleton for physical rehabilitation," *IEEE Trans. Robot.* **29**(1), 220–235 (2013).
29. M. Zinn, B. Roth, O. Khatib and J. K. Salisbury, "A new actuation approach for human friendly robot design," *Int. J. Robot. Res.* **23**(4-5), 379–398 (2004).
30. N. Vitiello, T. Lenzi, S. M. M. De Rossi, S. Roccella and M. C. Carrozza, "A sensorless torque control for Antagonistic Driven Compliant Joints," *Mechatronics* **20**(3), 355–367 (2010).
31. L. Bassi Luciani, V. Genovese, V. Monaco, L. Odetti, E. Cattin and S. Micera, "Design and evaluation of a new mechatronic platform for assessment and prevention of fall risks," *J. Neuroeng. Rehabil.* **9**(1), 51 (2012).
32. R. B. Davis, S. Ounpuu, D. Tyburski and J. R. Gage, "A gait analysis data collection and reduction technique," *Hum. Mov. Sci.* **10**, 575–587 (1991).
33. N. Vitiello, T. Lenzi, S. M. M. De Rossi, F. Giovacchini, M. Cempini and M. C. Carrozza, "Technological Aid for Transfemoral Amputees," PCT patent application number: PCT/IB2013/055065, Application date: June 20, 2013, Publication date: December 27, 2013, WO 2013/190495.
34. F. Zhang, S. E. D'Andrea, M. J. Nunnery, S. M. Kay and H. Huang, "Towards design of a stumble detection system for artificial legs," *IEEE Trans. Neural Syst. Rehabil. Eng.* **19**(5), 567–577 (2011).
35. D. A. Winter, *Biomechanics and Motor Control of Human Gait: Normal, Elderly and Pathological* (University of Waterloo Press, Waterloo, 1991).